

Miniaturized 180° Hybrid Coupler in LTCC for L-Band Applications

Greg Brzezina, *Member, IEEE*, and Langis Roy, *Member, IEEE*

Abstract—In this letter, the lumped element technique is used to design a 180° hybrid coupler or balun for applications at L1 band. The material system employed is low temperature co-fired ceramic (LTCC), which allows for three-dimensional passive integration. The proposed balun uses a modified equivalent circuit that permits the simultaneous optimization of amplitude and phase balances. A process for the quick tuning of the balun design parameters is also presented. Measurements at 1.575 GHz indicate insertion losses below 0.67 dB, an amplitude imbalance of 0.14 dB, and a phase difference of 179.1°. To the author's best knowledge, this is the smallest and best performing lumped element balun for applications at L1 band.

Index Terms—Couplers, LTCC.

I. INTRODUCTION

180° hybrids can be used as baluns to convert single-ended or unbalanced signals to differential or balanced equivalents. An ideal balun introduces a 180° phase shift at its output terminals and also divides the input power equally. Baluns are often placed between single ended filters and balanced mixers, amplifiers or antenna feed networks.

The conventional approach has been to use coupled lines (microstrip, stripline, etc.) to implement such a balun. This approach can yield low loss, broadband devices that are simple to design and manufacture. However, due to its electrical length, the size of the balun is often too large to be of practical use except at millimeter frequencies [1]. Smaller sizes can be achieved by using multi-layered substrates with spiral or folded line topologies and lumped loading [2]. The tradeoffs are reduced performance and smaller operating bandwidths due to the comparatively simple circuit topologies employed.

With about the same operating bandwidth of the loaded case, further miniaturization is possible if the entire balun is implemented with lumped elements [3]. Simplified networks can be realized with extremely small dimensions but they display even narrower bandwidth or poor phase balance [4]. Moreover, simplified networks make it difficult to optimize the amplitude and phase balance simultaneously due to the reduced number of design variables [5].

Manuscript received November 20, 2013; accepted February 26, 2014. Date of publication March 20, 2014; date of current version May 06, 2014.

The authors are with the Department of Electronics, Carleton University, Ottawa, ON K1S 5B6, Canada (e-mail: gbrzezina@doe.carleton.ca; lroy@doe.carleton.ca).

Color versions of one or more of the figures in this paper are available online at <http://ieeexplore.ieee.org>.

Digital Object Identifier 10.1109/LMWC.2014.2310469

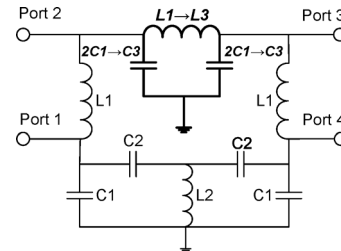


Fig. 1. Symmetric lumped element equivalent model for rat-race coupler (with modifications in bold).

In this letter, a new fully embedded lumped element balun is designed and characterized, which has the smallest dimensions reported to date when guided wavelength is considered. Its low insertion loss and accurate phase difference make it an ideal candidate for custom System-on-Package (SoP) transceivers for GPS, GLONASS, or Galileo satellite navigation systems.

II. SPECIFICATIONS AND CIRCUIT SCHEMATIC

The balun operates by introducing a 180° phase difference between the output ports (2 and 4) when power is applied to port 1. Meanwhile, port 3 remains isolated. Three 90° pi networks are inserted between ports 1–2, 2–3 and 3–4, while a 270° (or –90°) highpass tee network is placed between ports 1–4. The lumped equivalent model of the balun is shown in Fig. 1, with modifications indicated in bold to be described later. The corresponding design equations follow [(1)–(4)] [6]:

$$L1 = \frac{\sqrt{2}Z_0 \sin \theta}{\omega} \quad (1)$$

$$L2 = \frac{-\sqrt{2}Z_0}{\omega \sin \theta} \quad (2)$$

$$C1 = \frac{1}{\sqrt{2}Z_0\omega} \sqrt{\frac{1 - \cos \theta}{1 + \cos \theta}} \quad (3)$$

$$C2 = \frac{1}{\sqrt{2}Z_0\omega} \sqrt{\frac{1 + \cos \theta}{1 - \cos \theta}} \quad (4)$$

The lumped element values are obtained by substituting Z_0 with 50 Ω and ω with $2\pi \times 1.575 \times 10^9$ in all equations, while θ is substituted with 90° in (1) and (3). In (2) and (4), θ is replaced with –90°. The balun is designed to have a centre frequency of 1.575 GHz and 10 dB bandwidth of over 100 MHz. Insertion losses are to be kept as low as possible and an isolation of better than 20 dB is desired. Performing the calculations yields 7.15 nH for both $L1$ and $L2$ and 1.43 pF for both $C1$ and $C2$.

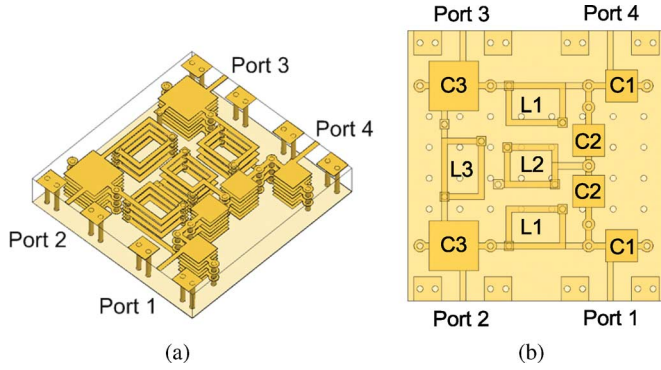


Fig. 2. Balun structure: (a) three dimensional view; and (b) top view.

TABLE I
BALUN OPTIMIZATION RESULTS (DIMENSIONS IN μm)

	<i>C3</i>	<i>C1</i> & <i>C2</i>	<i>L1</i>	<i>L2</i>	<i>L3</i>
Initial	630	450	500	500	500
Final	810	525	625	525	650

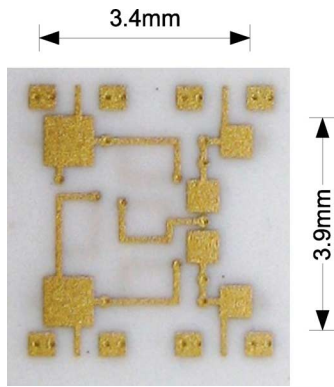


Fig. 3. Micrograph of fabricated LTCC balun.

III. BALUN DESIGN AND TUNING

The design of the balun follows the methodology described in [7], where a library of individual components is created and then used to systematically assemble the complete balun. The three-dimensional balun structure, shown in Fig. 2, uses techniques first presented in [8] but implements a different, higher density layout with all new components to create an original design. In this figure, individual capacitors and inductors are labeled so that a comparison with the schematic representation can be made.

The balun occupies only $3.9 \times 3.41 \times 0.679 \text{ mm}^3$ or $0.049 \times 0.043 \times 0.008 \lambda_0^3$ of a FerroA6 LTCC substrate (seven layers) that has a relative permittivity of 5.7 and loss tangent of 0.002. Silver is the conductor with gold plating on the outer layers. As can be seen in Fig. 2(a), the structure is very dense. The novel layout and packaging of the balun allows for an extreme degree of miniaturization that is unmatched in the literature when guided wavelengths are considered. In general, the topology of the model follows that of the schematic closely. However, a key reason for the model's compactness is that inductor $L2$ is folded inside and resides at the center of the balun structure (unlike in the schematic representation). In an effort to minimize resistive losses in the network, the number of vias used was reduced by combining as many nodes as possible.

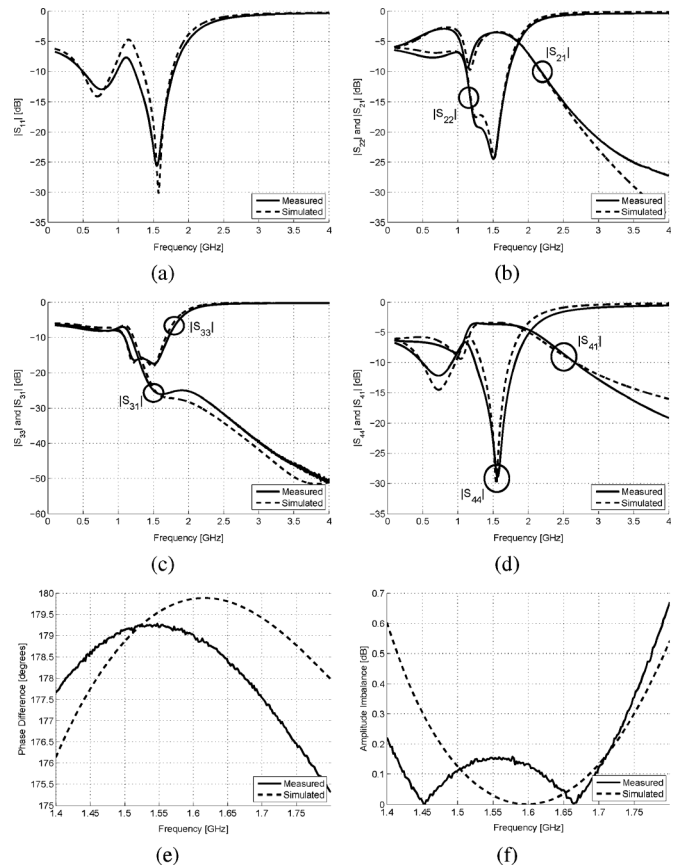


Fig. 4. Simulated and measured balun performance: (a) S_{11} ; (b) S_{22} and S_{21} ; (c) S_{33} and S_{31} ; (d) S_{44} and S_{41} ; (e) phase difference; and (f) amplitude imbalance.

To reduce the difficulty of optimizing the performance of the balun, modifications were made to the equivalent circuit (indicated in bold in Fig. 1) by making the component values of the pi network independent from the others. Designating $C3$ and $L3$ allows for the simultaneous optimization of amplitude and phase balances, which can be easily verified by any circuit simulator. This method is especially useful because it is valid for both schematic and 3-D representations of the design. Given these new degrees of freedom, a tuning process was developed to quickly determine all component values. Through the perturbation of one component value at a time the following behaviors were observed:

- 1) $C1$ and $C2$ have a strong effect on the center frequency. Increasing both reduces the balun's center frequency.
- 2) Increasing $C3$ reduces the output phase without significantly impacting the other parameters.
- 3) Changing $L2$ has a strong influence on output phase without greatly affecting amplitude balance.
- 4) Increasing the inductance between ports 2 and 3 ($L3$) reduces S_{41} and vice-versa.
- 5) Increasing the inductance between ports 1–2 and 3–4 ($L1$) increases S_{41} and vice-versa.

With this knowledge, the most effective methodology to tune the balun was found to be as follows: first, the center frequency of the balun was set by adjusting capacitors $C1$, $C2$ and $C3$; second, the amplitude balance was improved by adjusting the $L1$ inductors; third, $L2$ was changed to achieve the correct phase shift; lastly, $C3$ and $L3$ were used to make small adjustments to

TABLE II
BALUN MEASUREMENT SUMMARY

Item	Simulated	Measured	
		1575 MHz	1600 MHz
Center Freq.	1575 MHz	1575 MHz	1600 MHz
$ S_{21} $	-3.4 dB	-3.53 dB	-3.55 dB
$ S_{41} $	-3.4 dB	-3.67 dB	-3.68 dB
Phase Diff.	179.5 ⁰	179.1 ⁰	179 ⁰
Phase. Imb. [$f_c \pm 50$ MHz]	0.2 ⁰	0.4 ⁰	0.5 ⁰
Amp. Imb. [$f_c \pm 50$ MHz]	0.008 dB	0.14 dB	0.13 dB

TABLE III
COMPARISON WITH RELATED WORK

Ref.	ΔA (dB)	$\Delta\phi$ (deg.)	Vol. (λ_g^3)
[This work]	0.14	0.9	1.78×10^{-5}
[3]	0.3	8	2.03×10^{-5}
[8]	0.15	2.6	2.92×10^{-5}
[9]	0.4	5	3.38×10^{-5}
[5]	0.7	5	7.51×10^{-5}
[10]	0.05	1.9	7.69×10^{-5}
[4]	~ 0.1	N/A	8.88×10^{-5}
[2]	2.4	0.19	1.19×10^{-4}

the phase and amplitude balances. The final dimensions of each component were optimized in 17 iterations of manual tuning, which is much faster than what can be achieved by automatic optimizers. Table I shows the initial and final values.

IV. BALUN CHARACTERIZATION

The prototype balun was fabricated at the facilities of VTT Electronics in Oulu, Finland and is shown in Fig. 3. The measurement setup includes 500 μm pitch G-S-G probes that were calibrated to 50 Ω using the Short-Open-Load-Through (SOLT) technique to obtain 2-port S-parameter data (a 4-port test setup was not available). The remaining two ports were loaded with 50 Ω chip resistors. To obtain the full set of S-parameter data, three measurement configurations were required. The amplitude imbalance is calculated by subtracting the magnitudes of S_{41} and S_{21} , while the phase difference is obtained by subtracting their phases. A comparison of the simulated and measured results is shown in Fig. 4 with good agreement in all cases.

Measurements indicate impedance bandwidths at all ports of 500 MHz or 32% (from 1.2 to 1.7 GHz). At 1.575 GHz, insertion losses at the outputs are less than 0.67 dB and the phase difference is 179.1⁰, while the amplitude imbalance is

0.14 dB. A detailed summary of results is presented in Table II, while a comparison in terms of size in guided wavelengths with state-of-art lumped element baluns is made in Table III and sorted by volume (top—smallest) [9], [10]. For completeness, amplitude imbalance (ΔA) and phase imbalance ($\Delta\phi$) for each design are also listed.

V. CONCLUSION

This work has presented a new high performance balun with an extreme degree of miniaturization achieved with the lumped element technique. A modified equivalent circuit and design methodology were presented that allowed for fast tuning of the design. Standard, low permittivity LTCC substrate material was used to create a prototype with measured insertion losses below 0.67 dB, an amplitude imbalance of 0.14 dB and a phase difference of 179.1⁰ at 1.575 GHz. The performance of this balun compares very favorably with the state-of-art and confirms the usefulness of the proposed design methodology. Therefore, the new balun is a good choice for GPS, GLONASS, or Galileo satellite navigation systems.

ACKNOWLEDGMENT

The authors would like to thank K. Kautio, VTT Electronics, for his advice pertaining to LTCC fabrication, and A. Momciu, Communications Research Centre, for his help in characterizing the balun.

REFERENCES

- [1] N. Kidera, S. Pinel, S. Watanabe, K. Watanabe, and J. Laskar, "Wide-band, low loss and compact 3D LTCC balun with asymmetric structure for millimeter wave applications," *IEEE Trans. Microw. Theory Tech.*, vol. 3, pp. 547–550, Jun. 2005.
- [2] T. Yang, M. Tamura, and T. Itoh, "Compact and high-performance low-temperature co-fired ceramic balun filter using the hybrid resonator and symmetric four-port network," *IET Microw., Antennas Propag.*, vol. 6, no. 2, pp. 121–126, 2011.
- [3] T.-M. Shen, C.-R. Chen, T.-Y. Huang, and R.-B. Wu, "Design of lumped rat-race coupler in multilayer LTCC," in *Proc. Asia Pacific Microw. Conf.*, Dec. 2009, pp. 2120–2123.
- [4] R. Perrone, P. Kapitanova, D. Kholodnyak, I. Vendik, S. Humbla, M. Hein, and J. Müller, "Miniaturisation of a LTCC high-frequency rat-race-ring by using 3-dimensional integrated passives and embedded high-K capacitors," in *Proc. Eur. Microelectron. Packag. Conf.*, Jun. 2009, pp. 1–6.
- [5] S. Sakhnenko, D. Orlenko, K. Markov, A. Yatsenko, B. Vorotnikov, G. Sevskiy, P. Heide, and M. Vossiek, "Low profile LTCC balanced filter based on a lumped elements balun for WiMAX applications," *IEEE Trans. Microw. Theory Tech.*, pp. 1111–1114, Jun. 2008.
- [6] I. Bahl, *Lumped Elements for RF and Microwave Circuits*. Norwood, MA: Artech House, 2003.
- [7] G. Brzezina, L. Roy, and L. MacEachern, "Design enhancement of miniature lumped-element LTCC bandpass filters," *IEEE Trans. Microw. Theory Tech.*, vol. 57, no. 4, pp. 815–823, Jun. 2009.
- [8] G. Brzezina and L. Roy, "A miniature lumped element LTCC quadrature hybrid coupler for GPS applications," in *Proc. IEEE Antennas Propag. Symp.*, July 2008, pp. 1–4.
- [9] I. Piekarczyk, J. Sorocki, K. Wincza, S. Gruszczynski, J. Muller, and T. Welker, "Miniaturized quasi-lumped coupled-line single-section directional coupler designed in multilayer LTCC technology," *Microw. Opt. Technol. Lett.*, vol. 55, no. 6, pp. 1401–1405, Mar. 2013.
- [10] G.-S. Huang, C.-H. Wu, and C. H. Chen, "LTCC balun bandpass filters using dual-response resonators," *IEEE Microw. Wireless Compon. Lett.*, vol. 21, no. 9, pp. 483–485, Sep. 2011.